天文研究所
Institute of Astronomy

Unveiling the properties of star-forming galaxy populations in the γ–ray sky

國立清華大學
NATIONAL TSING HUA UNIVERSITY

Ellis R. Owen[1,2]
[1]Institute of Astronomy, National Tsing Hua University, Hsinchu, Taiwan (ROC)
[2]Center for Informatics and Computation in Astronomy, National Tsing Hua University, Hsinchu, Taiwan (ROC)

1 Introduction

Several nearby star-forming galaxies (SFGs) have been detected in γ-rays in recent years (Ajello et al. 2020), establishing such systems as a candidate source class for the extra-galactic γ-ray background (EGB); see also **Figure 1**. Their γ-ray emission is driven by an abundant reservoir of cosmic rays (CRs) which interact with interstellar gases to form pions and, subsequently, γ-rays. The production of secondary electrons, which thermalize quickly to deliver feedback heating arises alongside the γ-ray production. Thus, the EGB can be used to probe CR feedback in galaxies.

$$\mathrm{p+p} \rightarrow \begin{cases} \mathrm{p+p+}\pi^0 \\ \mathrm{n+p+}\pi^+ \\ \mathrm{p+p+}\pi^+ + \pi^- \end{cases} \qquad \pi^0 \rightarrow 2\gamma$$

+ pion multiplicities at higher energies

Pions decay to photons, muons, neutrinos, electrons, positrons, antineutrinos

The CRs within these systems are presumably accelerated by diffusive shock acceleration processes (e.g. Fermi 1949), boosting low energy charged seed particles to relativistic energies, operating in an abundance of violent shocked astrophysical environments. Such environments would be associated with the stellar end-products that arise soon after the onset of star-formation. This underlies a relation between the star-formation rate (SFR) of a galaxy and its γ-ray luminosity (see **Figure 2**).

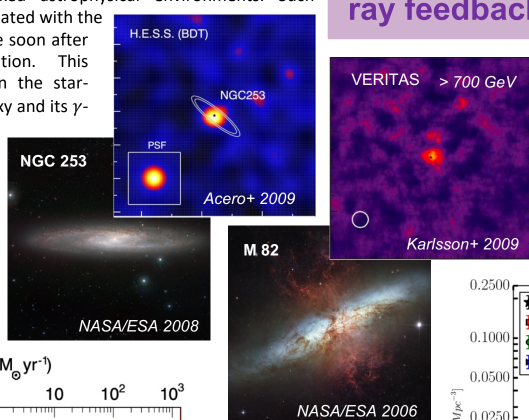

Figure 1 (right): *Examples of nearby SFGs detected in γ-rays, shown in optical/UV/H α and corresponding γ-ray significance maps. NGC 253 has a SFR of $\sim 10\,\mathrm{M_\odot yr^{-1}}$ while M82 presents a rate in the range $\sim(1-10)\mathrm{M_\odot yr^{-1}}$, i.e. about an order of magnitude higher than the Galaxy. The γ-ray luminosity correlates with the SFR.*

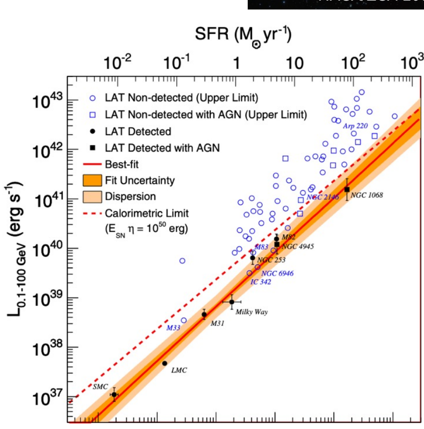

Figure 2 (left): *SFR- (0.1-100) GeV γ-ray relation showing good correspondence between γ-ray luminosity and SFR. This suggests the emission is driven by CR interactions, and is a useful tracer of CR feedback and energy deposition inside the host galaxy. Detected systems with Fermi-LAT are shown in black. Adapted from Ackermann et al. 2012.*

Contact

www.ellisowen.org

erowen@gapp.nthu.edu.tw

γ-ray emission has been detected from nearby star-forming galaxies in recent years, establishing such systems as a candidate source class for the extra-galactic γ-ray background. Contributions at different redshifts can be accessed using small-scale anisotropies in the γ-ray sky. These are sensitive to the peak of cosmic ray activity in low-mass starburst galaxies, and are a promising means to probe cosmic ray feedback at the noon of cosmic star-formation.

2 Prototype model

A prototype model was adopted to describe the CR containment and γ-ray emission spectrum from an individual galaxy, based on a limited number of parameters. The spectral density of CRs was obtained by solving the transport equation in the diffusion limit, with a renormalization based on an energy-dependent advective loss fraction (to account for the effect of galactic outflows in remoing CRs from their host galaxy). The spectral density of CRs in the SFG is then given by:

$$n_{\mathrm{p}}(\gamma_{\mathrm{p}})\,\mathrm{d}\gamma_{\mathrm{p}} = \frac{35R^2 f_{\mathrm{adv}}\,\mathcal{L}_0\,\mathcal{A}(\gamma_{\mathrm{p}})}{108\,D(\gamma_{\mathrm{p}})}\frac{\partial}{\partial\gamma_{\mathrm{p}}}\left(\frac{\gamma_{\mathrm{p}}}{\gamma_{\mathrm{p},0}}\right)^{-\Gamma}\mathrm{d}\gamma_{\mathrm{p}}\ ,$$

(Owen et al. 2022). Here, $f_{\mathrm{adv}} = 0.2$ accounts for the fraction of CRs lost to outflows (on average), $\mathcal{A}$ is the CR absorption fraction due to CR interactions arising within the host galaxy, D is the energy-dependent diffusion parameter (which quantifies the diffusive leaking of the CRs from a galaxy), R is the galaxy effective size (based on empirical scaling relations with SFR), and $\mathcal{L}_0$ is the CR luminosity (set by the SFR and CR production efficiency per supernova event, assuming 5% of stars formed yield a supernova event). $\Gamma = 2.1$ is the CR injection spectral index.

In this treatment CR containment is dependent on SFR, with stronger containment arising for CRs of higher energies within galaxies of higher SFR. This yields a γ-ray emission spectrum with hardness dependent on SFR. This is reflective of observations, and can reproduce the hardness-SFR γ-ray relation seen in nearby starburst galaxies (see **Figure 3**).

Free parameters in the protoype model for the γ-ray emission spectrum of a SFG are star-formation rate, stellar mass and redshift. These are provided by an input galaxy population model.

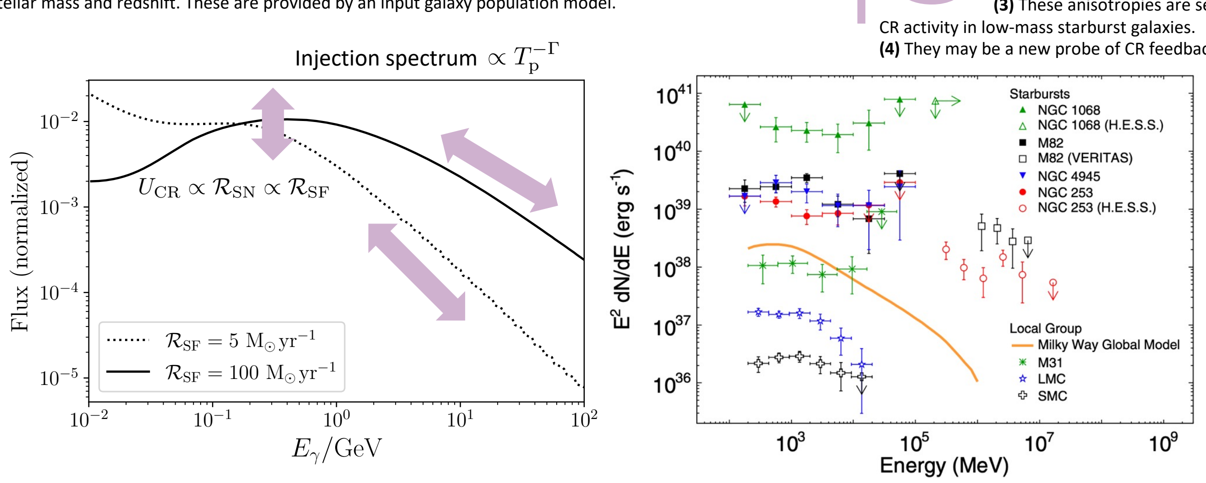

Figure 3, left panel: *Adapted from Owen et al. (2022), comparing two normalized γ-ray emission spectra for prototype galaxies with two SFRs. In absolute terms, the normalization of the spectrum would be proportional to the SFG of the galaxy, as indicated. The CR injection spectrum is the same in both cases, however the spectral hardening for higher SFRs results from more effective containment of higher-energy CR particles in our diffusive leaking treatment. This is reflective of the observed spectral behavior of nearby SFGs, shown on the right. The effects of internal γ-ray absorption through pair-production processes are fully included in the model, however this effect is relatively inconsequential at the energies shown here for the adopted parameter choices (this is not universally the case, as higher SFRs lead to stronger pair-production losses in this same energy range).* ***Right panel:*** *Adapted from Ackermann et al. (2012). This shows the observed spectra (or limits) for nearby SFGs. The relation between spectral normalization, hardness and SFR is evident from comparison with Figure 2.*

3 Galaxy populations

To obtain a model for the EGB, the prototype galaxy model was applied to the star-formation rate function and galaxy stellar mass functions obtained from the EAGLE simulations (for the specific relations used, see the 100N1504-Ref model of Katsianis et al. 2017). The corresponding cosmic star-formation rate density distribution of this galaxy population model is shown in **Figure 4**, which is broadly consistent with observational constraints. This shows that cosmic star-formation is dominated by strongly star-foming galaxies around the cosmic noon, with more quiescent galaxies being more important at later epochs.

To discern between main sequence star-forming galaxies, and galaxies undergoing intense starburst episodes, a starburst separation criteria was introduced. This defined starburst galaxies to be those experiencing star-formation at a rate that is 10 times higher than their lifetime average, i.e.

$$\mathcal{N}_{\mathrm{SF}}(t) = \mathcal{R}_{\mathrm{SF}}(t)/\langle\mathcal{R}_{\mathrm{SF}}\rangle_t \approx t\,\mathcal{R}_{\mathrm{SF}}(t)/M^\star$$

where $\mathcal{R}_{\mathrm{SF}}$ is the SFR of a galaxy, t is its age (defined simply as the age of the Universe at redshift z) and where M^* is the galaxy stellar mass. For starburst galaxies, we require that $\mathcal{N}_{\mathrm{SF}} > 10$. This criteria was in good agreement with a threshold of 20 times the main sequence of star-forming galaxies at $z{\sim}2$.

Figure 4 (below): *Cosmic star-formation rate density for the reference input galaxy evolution model obtained from the EAGLE simulations (see Katsianis et al. 2017 for details). The total star-formation rate density shown is approximately consistent with observations. The contribution from galaxies with different SFRs is indicated, with the peak of cosmic star-formation density (the so-called "noon" of star-formation) driven mainly by highly star-forming galaxies, and more quiescent galaxies dominating cosmic star-formation at later epochs.*

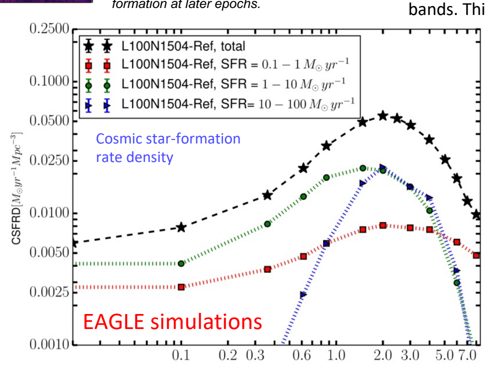

4 Results

By separating the contribution from starburst and main sequence SFGs, the star-forming galaxy contribution to the EGB was found to be **strongly dominated by starburst galaxies** at all energies. These provide around 93.7 % of the SFG contribution to the EGB at 0.01 GeV, rising to 99.7 % by 50 GeV. This is despite starbursts being substantially less numerous compared to main sequence SFGs.

The SFG contribution can be further separated. **Figure 5** shows the fractional contribution from SFGs distributed over redshift, with relative intensities from different types of galaxies split according to their stellar mass in six bands. This shows that (1) the SFG contribution to the EGB is **dominated by low mass galaxies**, with those of stellar mass below $10^9\,\mathrm{M_\odot}$ contributing over 95% of the intensity, and (2) that **most of the contribution originates from around and before the noon of cosmic star-formation**. This suggests that the EGB, if well-described by the model considered in this work, is most sensitive to CR activity in relatively small galaxies building up their stellar mass before the peak of cosmic star-formation. This indicates that studies of the EGB can be a useful means to probe the involvement of CR feedback in the structural evolution of galaxies at a time in cosmic history when they were undergoing the most significant phase of their development.

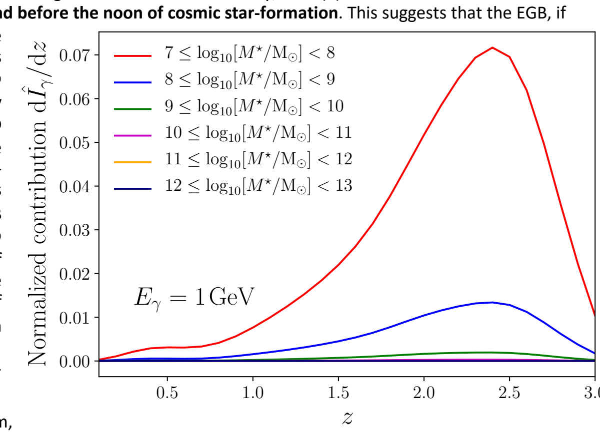

Figure 5 (above): *Redshift distribution of the intensity contribution to the EGB from star-forming galaxies. This is dominated by starburst galaxies, with the majority of the intensity originating from relatively low-mass galaxies. These are typically located slightly before the noon of cosmic star-formation and indicate the EGB in this model is a useful tracer of CR activities in galaxies just prior to the peak in cosmic star-formation, during the epoch when their feedback effects would be most severe. Most of the EGB contribution would originate in galaxy populations represented by the blue line in Figure 4.*

The spatial distribution of SFGs, set by their power spectrum, would imprint a spatial signature in the EGB, even though individual contributing sources would not typically be resolved. The distribution of spatial scales of this signature would depend on redshift, and the strength of the contribution from sources at a particular epoch. The imprinted signatures could be accessed in the EGB using the intensity fluctuation power spectrum (see **Figure 6**) providing an alternative window to study EGB source populations and their evolution over cosmic time. This could be used to gain crucial new insights about CR activity in EGB source populations and its co-evolution with galaxy populations. Our capability to resolve EGB anisotropies will be substantially improved with the continuing operation of *Fermi*-LAT, and the higher angular resolution afforded by the up-coming Cherenkov Telescope Array.

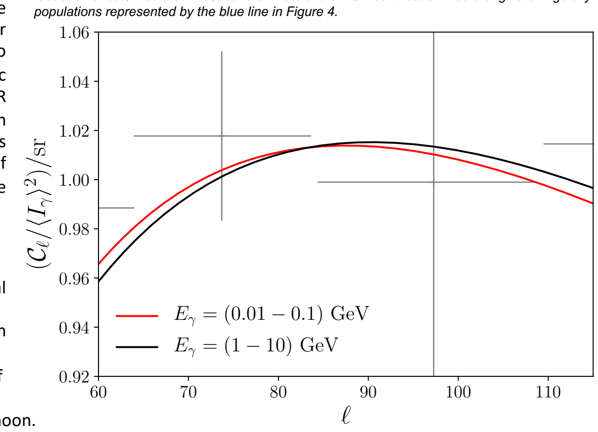

5 Conclusions

(1) Star-forming galaxies can make a substantial contribution to the diffuse γ-ray sky.
(2) Their contributions at different redshifts can be accessed using small-scale anisotropies.
(3) These anisotropies are sensitive to the peak of CR activity in low-mass starburst galaxies.
(4) They may be a new probe of CR feedback during the cosmic noon.

Figure 6 (above): *The strongly-peaked intensity contribution in redshift space (shown in Figure 5) can be measured using small-scale anisotropy signatures in the γ-ray sky. As a proof-of-concept model, this figure shows the anisotropy signature that results from the model considered in this work. The distribution of galaxies over cosmic time is set by the underlying matter power-spectrum. This is redshift-dependent and ensures that galaxies at a particular epoch imprint EGB signatures at a preferred length scale. Different source redshift distributions thus encode EGB signatures at distinctive angular scales. Comparison is made with observationally-derived constraints, using data obtained with Fermi-LAT by Fornasa et al. (2016).*

Further details

Owen, Lee & Kong 2021
MNRAS 506, 1, p.52
(arXiv: 2106.07308)

Owen, Kong & Lee 2022
MNRAS 513, 2, p. 2335
(arXiv: 2112.09032)

References: *Ackermann et al. 2012, ApJ 755, 164; Ajello et al. 2020, ApJ 894, 88; Fermi 1949 Phys. Rev. 75, 1169; Fornasa et al. 2016, Phys. Rev. D, 94, 123005; Katsianis et al. 2017 MNRAS 472, 919; Owen et al. 2021, MNRAS 506, 52; Owen et al. 2022, MNRAS 513, 2335*